COMMUNICATION

Check for updates

Point + Gaussian charge model for electrostatic interactions derived by machine learning

David van der Spoel ᴵᴰ * and A. Najla Hosseini ᴵᴰ

At short distances between atoms, point charges are a poor approximation of the electrostatic interaction. Due to overlapping electron clouds, charges are effectively shielded and the electrostatic interaction energy is modified. In molecular simulations, two main approaches have surfaced to deal with this. First, the Thole-screening [B. T. Thole, *Chem. Phys.*, 1981, 59, 341–350], which introduces a mathematical modification of the Coulomb interaction at short range, and second, the use of Gaussian-distributed charges [C. M. Smith and G. G. Hall, *Theor. Chim. Acta* 1986, 69, 63–69]. Here, we show that these approaches are practically equivalent, that is the screening functions are numerically very similar and their parameters related by a simple expression. A quantitative comparison between electrostatic interactions in alkali-halide ion pairs, computed using high level symmetry-adapted perturbation theory (SAPT), and in point charge models shows that the electrostatic interactions are not always weaker than those predicted by point charge approximations, highlighting that more complex atomic models may be needed. We then proceed to use machine learning with the Alexandria Chemistry Toolkit to train models for alkali-halides based on a positive core and a virtual site with a negative Gaussian-distributed charge and show that this model yields energies very close to SAPT.

Understanding the limitations of charge models is essential for accurately representing electrostatics in molecular systems. Standard point-charge approaches can overestimate dipole moments, particularly in systems with significant charge overlap or polarization effects. For instance, the experimental dipole of alkali halide ion-pairs at their minimum energy distance is 15–30% smaller than what would be expected from point charges (see Table S2 in ref. 1). This shows that charge penetration has to be taken into account when computing electrostatic interactions and several, relatively simple, modifications of the Coulomb equation can be used to incorporate this effect.

Dept. Cell and Molecular Biology, Uppsala University, Box 596, SE-75124 Uppsala, Sweden. E-mail: david.vanderspoel@icm.uu.se

In the early 1980s, Thole introduced a smeared interaction between point dipoles i and j at distance r_{ij} to better model short range interactions:[2]

$$S(r_{ij}) = 1 - \left(1 + \frac{r_{ij}}{2a}\right)\exp\left(-\frac{r_{ij}}{a}\right) \quad (1)$$

where

$$a = \frac{(\alpha_i \alpha_j)^{\frac{1}{6}}}{t} \quad (2)$$

in which the α are the polarizability volumes of the atoms i and j, and t is a dimensionless constant. This kind of function is used, for instance, in the CHARMM-Drude force field (FF) to screen the Coulomb interactions between divalent cations and water oxygen.[3]

Some years after the Thole paper, it was realized that both the electron density and the electrostatic potential generated by small molecules can be reproduced by a combination of point charges and a Gaussian-distributed charge.[4–6] The Coulomb interaction between two Gaussian-distributed charges q_i and q_j with screening widths ζ_i and ζ_j, respectively, is given by

$$V(r_{ij}) = \frac{q_i q_j}{4\pi\varepsilon_0 r_{ij}}\mathrm{erf}(\zeta_{ij} r_{ij}) \quad (3)$$

where ε_0 is the permittivity of vacuum and

$$\zeta_{ij} = \frac{\zeta_i \zeta_j}{\sqrt{\zeta_i^2 + \zeta_j^2}}. \quad (4)$$

The screening function due to the distributed charge hence equals $\mathrm{erf}(\zeta_{ij} r_{ij})$. Models featuring Gaussian-distributed charges have been studied at length over the last two decades.[1,7–12]

Both the Thole screening function (eqn (1)) and the error function in eqn (3) converge to 1 rapidly with increasing distance r. By integrating the difference between the functions from zero to infinity it is possible to approximate ζ in terms of a:

$$\zeta = \frac{2}{3a\sqrt{\pi}}. \quad (5)$$

This journal is © the Owner Societies 2025

Phys. Chem. Chem. Phys., 2025, **27**, 13817–13820 | **13817**

Fig. 1 Screening function due to Thole with polarizabilities α_i and α_j both set to α as indicated, and $t = 2.6$, compared to the screening due to two Gaussian-distributed charges with ζ as computed from eqn (5). Distance corresponds to r_{ij} in eqn (1) and (3).

Fig. 1 shows the effective screening functions due to Thole and Gaussian distributed charges for two typical atomic polarizabilities α[11] with ζ corresponding to eqn (5). Although not identical, these curves are very similar. Thole himself wrote[2] that "the use of the scaling distance (eqn (2)) is arbitrary". On the other hand, to describe the charge distribution of an atom by a single Gaussian is an oversimplification as well, that is insufficient for modeling the electron density around, for instance, a water molecule.[5] In short, there is no physics-based argument to prefer one or the other description.

It is tempting to compare screened Coulomb functions to real electrostatic interactions as can be computed using SAPT.[13,14] Based on the ratio of the SAPT electrostatic energy component and the Coulomb interaction between two point charges, ζ or a can be computed. Table 1 lists, for nine alkali halide ion-pairs, the energy corresponding to point charges (PC), and from SAPT. Then, ζ is computed from

$$r\zeta = \mathrm{erf}^{-1}\left(\frac{E_{\mathrm{SAPT}}}{E_{\mathrm{PC}}}\right) \qquad (6)$$

where the inverse error function was computed using Scientific Python.[15] a was computed using a bisection algorithm hand-coded in Python. Finally, ζ' in Table 1 is derived from a using

eqn (5). The keen reader will note that the electrostatic interaction between Li$^+$ and halides as computed by SAPT is indeed weaker than that of a pair of point charges, and hence both a and ζ can readily be analyzed. Intriguingly, the electrostatic interactions of Na$^+$ and K$^+$ with halide ions are *stronger* than those of a pair of point charges. The reason for this, is that real atoms consist of nucleus with an electron cloud, and at sufficiently close distance and sufficiently large nuclear charge, the sum of interactions will be stronger than that of a point charges.

The electrostatic energies computed by SAPT were compared to a polarizable alkali-halide model by Walz and co-workers.[1] Fig. 2 shows that the SAPT electrostatic energies for nine ion pairs and a range of distances are reproduced poorly by this relatively advanced model. Indeed, the Walz *et al.* model is quantitatively (ion pairs involving Li$^+$) and even qualitatively (ion pairs involving Na$^+$ or K$^+$) incorrect. The reason for this is, that core and shell share the same Gaussian screening width in this model, and hence the electrostatic interaction at short distance is weaker than a point charge, which is not consistent with SAPT for ion pairs involving Na$^+$ or K$^+$ (see also Table 1). Despite this, the model was found to be quite accurate in applications such as the prediction of molten salt properties, melting points, and conductivity[20-23] because it relies on error compensation between the energy components, like most classical FFs.[24,25] The CHARMM-Drude model for ions mentioned above[3] employs point charges and therefore yields the exact same electrostatic energy as a pair of point charges.

Taken together, this analysis suggests that FF models should be constructed from the combination of a positive point charge and a Gaussian-distributed "electron cloud" with a compensating negative charge. The latter can be implemented as a virtual site located at the ion position, such that the net charge is +1 for Na$^+$ and K$^+$ and -1 for the halide ions. Li$^+$ can be modeled as a point charge. The Alexandria Chemistry Toolkit (ACT)[25] was used to train such a model, by optimizing atomic charges and Gaussian distribution widths (ζ, eqn (4)) to reproduce the SAPT electrostatic interactions for all ion pairs at the same time. The resulting parameters are listed in Table 2.

The ACT point + Gaussian model yields energy curves that adhere closely to SAPT (Fig. 2). In fact, the ACT model is an order of magnitude more accurate than point charges or the model due to Walz *et al.*[1] (Table 3), showing that accuracy of force field electrostatics can be improved vastly over simple point charges.

In a recent review of the Open Force Field project, Wang *et al.* coined the term "Force Field Science" to describe the study of potential functions and algorithms in a systematic manner.[27] They went on to suggest that this new branch of computational chemistry was virtually unexplored. Indeed, systematic design of FFs[28] is needed and the long history of model building by hand[29,30] should be incorporated in these efforts. Our group has focused on highlighting the effect different potentials have on simulations for alkali halides,[1,20-23] for noble gases[31] and most recently on alcohol-water mixtures.[25] The introduction of the Alexandria Chemistry Toolkit[25] will

Table 1 Electrostatic energy for ion pairs close to the minimum energy distance computed using point charges (PC) and for electrostatics as computed using symmetry-adapted perturbation theory at the SAPT2+3(CCD)δMP2 level of theory[14] with the aug-cc-pvtz basis set,[16] except for potassium, where the def2-TZVPP basis set was used instead.[17] Energies were computed using the Psi4 suite of programs.[18] Details for computing a, ζ and ζ' are given in the running text

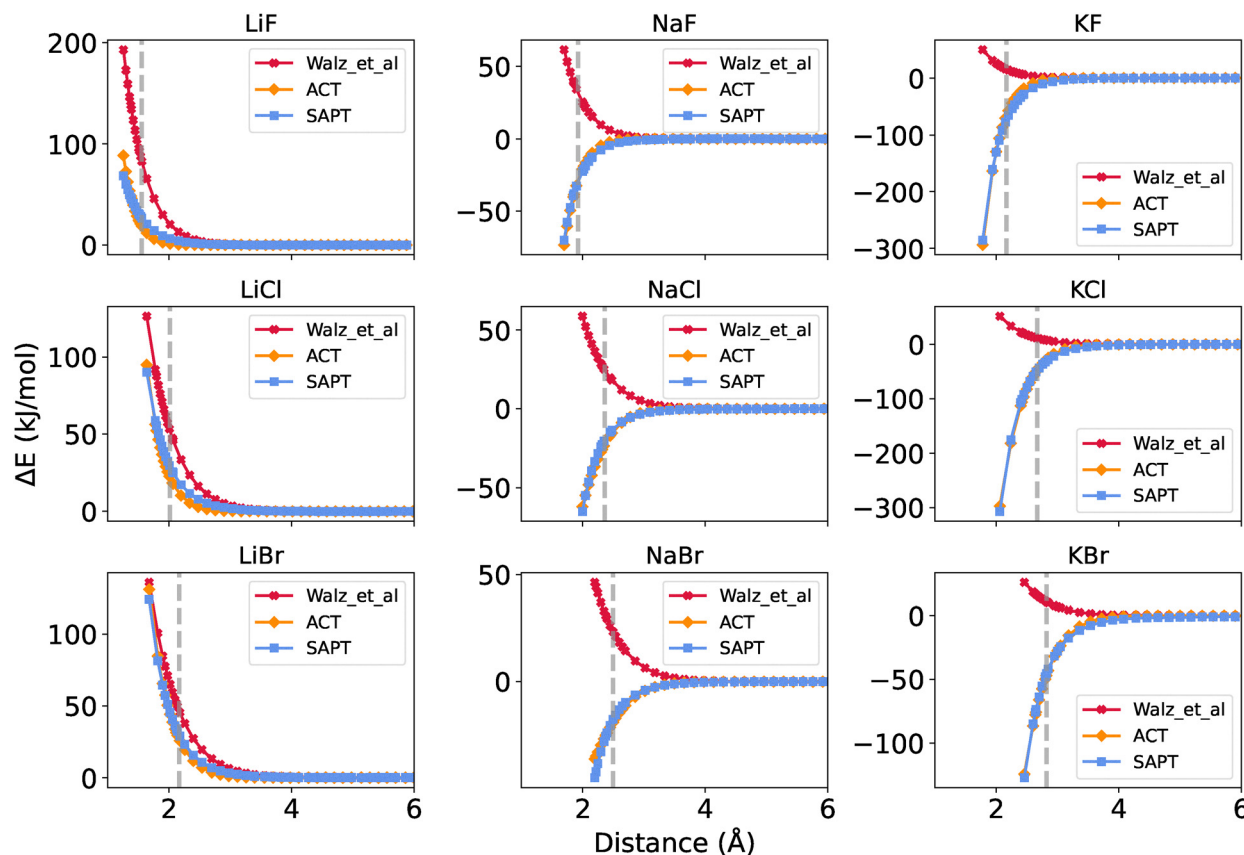|	r (nm)	E_{PC} (kJ mol^{-1})	E_{SAPT} (kJ mol^{-1})	a (nm)	ζ (nm^{-1})	ζ' (nm^{-1})
LiF	0.1640	−847.0	−826.4	0.03300	9.72	11.40
LiCl	0.2060	−674.3	−648.7	0.04638	7.12	8.11
LiBr	0.2260	−614.6	−591.8	0.05061	6.52	7.43
NaF	0.2020	−687.6	−708.8	—	—	—
NaCl	0.2480	−560.1	−573.8	—	—	—
NaBr	0.2540	−546.9	−562.6	—	—	—
KF	0.2260	−614.6	−667.9	—	—	—
KCl	0.2760	−503.3	−540.1	—	—	—
KBr	0.2820	−492.6	−538.1	—	—	—

Fig. 2 Difference between electrostatic energy from SAPT2+3(CCD)δMP2/aug-cc-pVTZ, the Walz *et al.* model (Gaussian), and ACT (positive point charge + negative Gaussian + distributed charge) and the interaction of two point charges. For calculations of interaction involving the model for alkali halides due to Walz *et al.*,[1] the exact same charges and ζ were used as in the original study. Where positive (ion-pairs involving Li$^+$), the interaction is weaker than that between a pair of point charges and *vice versa*. Dashed lines indicate the minimum energy distances from gas-phase experimental data[19]: LiF (1.56 Å), LiCl (2.02 Å), LiBr (2.17 Å), NaF (1.93 Å), NaCl (2.36 Å), NaBr (2.50 Å), KF (2.17 Å), KCl (2.67 Å), and KBr (2.82 Å).

Table 2 Charges for the core (C) and virtual sites (VS) in the point + Gaussian model. ζ is the Gaussian distribution width. To determine these parameters, the hybrid Genetic Algorithm/Monte Carlo (GA/MC) approach in the ACT[25] was used with a population size of 128 over twenty generations. Each generation consisted of 40 Monte Carlo iterations, with a "temperature" of 0.01[26]

Parameter	q_C	q_{VS}	ζ_{VS} (nm^{-1})
F$^-$	1.24604	−2.24604	11.7866
Cl$^-$	1.84001	−2.84001	8.87883
Br$^-$	1.488	−2.488	7.80382
Li$^+$	1	—	—
Na$^+$	5.70319	−4.70319	20.4367
K$^+$	9.80622	−8.80622	14.1548

Table 3 RMSD values (kJ mol^{-1}) for the Walz *et al.* model (Gaussian), Point charge (PC), and ACT (point charge + Gaussian virtual sites) with respect to SAPT2+3(CCD)δMP2/aug-cc-pVTZ energies computed over the whole curve plotted in Fig. 2

Compound	Walz *et al.*	PC	ACT
LiF	36.2	18.6	3.9
LiCl	13.6	22.0	3.1
LiBr	10.1	30.0	2.0
NaF	32.0	16.2	1.1
NaCl	32.5	16.0	1.2
NaBr	28.2	13.2	1.8
KF	64.5	54.2	4.2
KCl	68.0	57.2	2.4
KBr	39.4	32.2	1.4
Average	40.4	32.1	2.7

make it easy to perform Force Field Science experiments by deriving FFs using different potentials and charge models from scratch with the purpose to critically evaluate their properties.[32,33] As we show here, both Thole screening and Gaussian-distributed charges give very similar reduction of the interaction strength at short distance and the complexity of the eqn (3) and (1) is similar as well. A careful analysis of the chemistry involved (Table 1 and Fig. 2) shows, however, that charge interactions can

be more complex than that given by just (screened) Coulomb interactions. For the alkali halide ion pairs studied here, the still relatively simple combination of a point charge and a Gaussian charge distribution provides an order of magnitude more accurate rendering of the electrostatic interactions than previous models. Further research is needed to determine whether such a

This journal is © the Owner Societies 2025

Phys. Chem. Chem. Phys., 2025, **27**, 13817–13820 | **13819**

model is needed for all atoms, or just a subset. The Alexandria Chemistry Toolkit can be used for this kind of studies in Force Field Science.[25,34]

Author contributions

DvdS conceived the study and wrote the first version of the manuscript. He created scripts to produce Fig. 1 and Table 1. ANH made suggestions to extend the work, performed calculations, compiled Tables 2, 3 and Fig. 2 and she contributed to writing.

Conflicts of interest

There are no conflicts to declare.

Data availability

All scripts and SAPT datasets are openly available on **https://github.com/AlexandriaChemistry/Data/GitHub**.

Notes and references

1 M. M. Walz, M. M. Ghahremanpour, P. J. van Maaren and D. van der Spoel, *J. Chem. Theory Comput.*, 2018, **14**, 5933–5948.
2 B. T. Thole, *Chem. Phys.*, 1981, **59**, 341–350.
3 H. Yu, T. W. Whitfield, E. Harder, G. Lamoureux, I. Vorobyov, V. M. Anisimov, A. D. MacKerell, Jr. and B. Roux, *J. Chem. Theory Comput.*, 2010, **6**, 774–786.
4 G. G. Hall and C. M. Smith, *Int. J. Quantum Chem.*, 1984, **25**, 881–890.
5 C. M. Smith and G. G. Hall, *Theor. Chim. Acta*, 1986, **69**, 63–69.
6 G. G. Hall and K. Tsujinaga, *Theor. Chim. Acta*, 1986, **69**, 425–436.
7 D. Elking, T. Darden and R. J. Woods, *J. Comput. Chem.*, 2007, **28**, 1261–1274.
8 D. M. Elking, G. A. Cisneros, J.-P. Piquemal, T. A. Darden and L. G. Pedersen, *J. Chem. Theory Comput.*, 2010, **6**, 190–202.
9 P. T. Kiss, P. Bertsyk and A. Baranyai, *J. Chem. Phys.*, 2012, **137**, 194102–194111.
10 P. T. Kiss and A. Baranyai, *J. Chem. Phys.*, 2014, **141**, 114501.
11 M. M. Ghahremanpour, P. J. van Maaren, C. Caleman, G. R. Hutchison and D. van der Spoel, *J. Chem. Theory Comput.*, 2018, **14**, 5553–5566.
12 L. Zhang, H. Wang, M. C. Muniz, A. Z. Panagiotopoulos, R. Car and W. E, *J. Chem. Phys.*, 2022, **156**, 124107.
13 B. Jeziorski, R. Moszynski and K. Szalewicz, *Chem. Rev.*, 1994, **94**, 1887–1930.
14 T. M. Parker, L. A. Burns, R. M. Parrish, A. G. Ryno and C. D. Sherrill, *J. Chem. Phys.*, 2014, **140**, 094106.
15 P. Virtanen, R. Gommers, T. E. Oliphant, M. Haberland, T. Reddy, D. Cournapeau, E. Burovski, P. Peterson, W. Weckesser, J. Bright, S. J. van der Walt, M. Brett, J. Wilson, K. J. Millman, N. Mayorov, A. R. J. Nelson, E. Jones, R. Kern, E. Larson, C. J. Carey, İ. Polat, Y. Feng, E. W. Moore, J. VanderPlas, D. Laxalde, J. Perktold, R. Cimrman, I. Henriksen, E. A. Quintero, C. R. Harris, A. M. Archibald, A. H. Ribeiro, F. Pedregosa and P. van Mulbregt, SciPy 1.0 Contributors, *Nat. Methods*, 2020, **17**, 261–272.
16 T. H. Dunning, Jr. and K. A. Peterson, *J. Chem. Phys.*, 2000, **1113**, 7799–7808.
17 F. Weigend and R. Ahlrichs, *Phys. Chem. Chem. Phys.*, 2005, **7**, 3297.
18 J. M. Turney, A. C. Simmonett, R. M. Parrish, E. G. Hohenstein, F. A. Evangelista, J. T. Fermann, B. J. Mintz, L. A. Burns, J. J. Wilke, M. L. Abrams, N. J. Russ, M. L. Leininger, C. L. Janssen, E. T. Seidl, W. D. Allen, H. F. Schaefer, R. A. King, E. F. Valeev, C. D. Sherrill and T. D. Crawford, *Wiley Interdisc. Rev.: Comput. Mol. Sci.*, 2011, **2**, 556–565.
19 F. Lovas, Diatomic Spectral Database, NIST Standard Reference Database 114, 2002, **https://www.nist.gov/pml/data/msd-di/index.cfm**.
20 M.-M. Walz and D. van der Spoel, *Phys. Chem. Chem. Phys.*, 2019, **21**, 8516–18524.
21 M.-M. Walz and D. van der Spoel, *Chem. Commun.*, 2019, **55**, 12044–12047.
22 M.-M. Walz and D. van der Spoel, *J. Phys. Chem. C*, 2019, **123**, 25596–25602.
23 M.-M. Walz and D. van der Spoel, *Commun. Chem.*, 2021, **4**, 1–10.
24 M. Zgarbova, M. Otyepka, J. Sponer, P. Hobza and P. Jurecka, *Phys. Chem. Chem. Phys.*, 2010, **12**, 10476–10493.
25 D. van der Spoel, J. Marrades, K. Kříž, A. N. Hosseini, A. T. Nordman, J. P. A. Martins, M.-M. Walz, P. J. van Maaren and M. M. Ghahremanpour, Evolutionary Machine Learning of Physics-Based Force Fields in High-Dimensional Parameter-Space, *chemrxiv*, 2025, preprint, chemrxiv:2025-0tw95, DOI: **10.26434/chemrxiv-2025-0tw95**.
26 D. van der Spoel, P. J. van Maaren and M. M. Ghahremanpour, *Alexandria Chemistry Toolkit Reference and User Manual version 1.0*, The Alexandria Chemistry Project, Uppsala, Sweden, 2025.
27 L. Wang, P. K. Behara, M. W. Thompson, T. Gokey, Y. Wang, J. R. Wagner, D. J. Cole, M. K. Gilson, M. R. Shirts and D. L. Mobley, *J. Phys. Chem. B*, 2024, **128**, 7043–7067.
28 D. van der Spoel, *Curr. Opin. Struct. Biol.*, 2021, **67**, 18–24.
29 P. Dauber-Osguthorpe and A. T. Hagler, *J. Comput. Aid. Mol. Des.*, 2019, **33**, 133–203.
30 A. Hagler, *J. Comput. Aid. Mol. Des.*, 2019, **33**, 205–264.
31 K. Kříž, P. J. van Maaren and D. van der Spoel, *J. Chem. Theory Comput.*, 2024, **20**, 2362–2376.
32 W. F. van Gunsteren and A. E. Mark, *J. Chem. Phys.*, 1998, **108**, 6109–6116.
33 D. van der Spoel, J. Zhang and H. Zhang, *Wiley Interdisc. Rev.-Comput. Mol. Sci.*, 2022, **12**, e1560.
34 K. Kříž and D. van der Spoel, *J. Phys. Chem. Lett.*, 2024, **15**, 9974–9978.

13820 | *Phys. Chem. Chem. Phys.*, 2025, **27**, 13817–13820

This journal is © the Owner Societies 2025